Journal of Russian Laser Research, Volume 24, Number 1, 2003

LOW-TEMPERATURE ANTI-STOKES LUMINESCENCE IN $Zn_{1-x}Mg_xSe$ MIXED CRYSTALS

A. A. Belov[1], F. Firszt[2], V. S. Gorelik[1], A. L. Karuzskii[1], E. I. Mahov[1], H. Męczyńska[2], A. V. Perestoronin[1], P. P. Sverbil[1], and J. Szatkowski[2]

[1]*P. N. Lebedev Physical Institute, Russian Academy of Sciences, Leninskii Pr. 53, Moscow 119991, Russia*
[2]*Institute of Physics, N. Copernicus University, Grudziądzka 5/7, 87-100 Toru, Poland*
e-mail: karuz@sci.lpi.msk.su

Abstract

Investigations of photoluminescence and Raman scattering in the ternary $Zn_{1-x}Mg_xSe$ compounds at 4.2 K were performed both in the Stokes and anti-Stokes regions using cw laser excitation with various wavelengths within the transparency band of the crystals. The anti-Stokes luminescence was observed for the first time in the ternary $Zn_{1-x}Mg_xSe$ compounds. We have found variations in the shape and position of the Stokes and anti-Stokes luminescence bands with an increase in the band gap energy, which depends on magnesium content. We assume that the anti-Stokes emission is generated by a two-step excitation via deep-level centers. It is shown that the low-temperature anti-Stokes photoluminescence can probe the spatial distribution profiles of impurities in the bulk of crystals.

Keywords: photoluminescence, Raman scattering, $Zn_{1-x}Mg_xSe$ compounds, deep-level centers.

1. Introduction

Electronic and vibrational properties of wide gap semiconductors are strongly determined by shallow- and deep-level centers, which are usually present due to impurities and defects. The composition and properties of the centers are related to the growth conditions of wide gap materials. Mixed crystals allow one to control the band gap energy by means of composition variation. The anti-Stokes luminescence was found in wide gap semiconductors, which possess impurities and defects [1–4]. If the photon energy of the incident exciting radiation E_0 is greater than the band gap of the semiconductor or insulator, the secondary radiation (photoluminescence and Raman scattering) occurs only in a thin subsurface layer. As a result, the analysis of the photoluminescence (PL) and Raman scattering spectra in this case provides information on electronic and vibrational properties just for this thin layer of the material. If the exciting photon energy E_0 is lower than the energy gap, the secondary radiation both in Stokes ($E < E_0$) and anti-Stokes ($E > E_0$) regions originates in the bulk of the sample. In this case, the emission from the sample can arise as the photoluminescence caused by both surface and bulk impurity centers. The volume anti-Stokes PL (APL) can be due to a two-step optical excitation of the energy levels involving the impurity centers. The anti-Stokes secondary radiation can also be caused by the following processes in condensed matter when excited by an intense pulsed source of light: two-photon excited luminescence, hyper-Raman and hyper-Raleigh scattering, second- and mixed-harmonic generation, and multiphoton

Translated from a manuscript submitted November 14, 2002.

 1071-2836/03/2401-0014$25.00

processes. Given the relatively low intensity of the excitation sources used in our experiments, the latter mechanisms will be beyond the scope of further considerations.

Anti-Stokes luminophors which have an anomalously high intensity of the APL are currently known [2–4]. A special class of anti-Stokes luminophors is presented by single crystals or glasses with rare earth elements (ytterbium, thulium, holmium, and others) as the impurity centers. The primary (exciting) radiation excites the long-lived electron states in such luminophors. Further excitation of these centers with subsequent APL may occur at the next stage. It has been found [1, 3, 5, 6] that, if the sample temperature is 4.2 K, the APL is present in all investigated samples, even in intentionally undoped and high-purity crystals. Since the presented technique of the volume excitation of the low-temperature secondary radiation spectra can be used in qualitative and quantitative analysis of both shallow- and deep-level centers in the bulk of the semiconductor, further detailed study of the excitation and APL emission in condensed matter is of interest.

The goal of this paper is to analyze the impurity and defect properties in the bulk of wide-gap semiconducting $Zn_{1-x}Mg_xSe$ mixed crystals by means of PL and Raman scattering spectroscopy at low temperatures.

2. Samples and Experimental

The base ZnSe compound is characterized by the spatial symmetry group T_d^2. It is a direct-gap semiconductor with a band gap of 2.67 eV at room temperature and 2.818 eV at a temperature of 4.2 K [7]. The APL at the temperature of 4.2 K was observed earlier in ZnSe single crystals as well as in a number of other II–VI compounds [1, 5, 6]. The APL of the ZnSe single crystal doped with Cr was studied in [3]. For ZnSe at a temperature of 4.2 K, the free exciton line energy is $E_g^{\text{ex}} = 2.802$ eV. For $Zn_{1-x}Mg_xSe$ with $x = 0.49$ it is equal to $E_g^{\text{ex}} = 3.385$ eV. With an increase in the Mg concentration x, the $Zn_{1-x}Mg_xSe$ band gap increases linearly [8]. We have performed measurements of the PL spectra of $Zn_{1-x}Mg_xSe$ ternary compounds both in the Stokes and anti-Stokes regions using continuous-wave laser excitation at various wavelengths within the transmission band of the crystals.

The ZnSe and ternary $Zn_{1-x}Mg_xSe$ compounds have been investigated at 4.2 K. The $Zn_{1-x}Mg_xSe$ mixed crystals with different compositions x were grown by the high-pressure Bridgman method under argon overpressure following the procedure described in [9]. The ZnSe purity was $6N$ and the Mg purity was $3N$. The crystals were cut into plates perpendicularly to the growth direction; they were mechanically polished and chemically etched. All samples used in this study were as-grown and not doped intentionally. During the crystal growth magnesium segregation occurred; therefore the actual sample composition was determined according to the position of the exciton photoluminescence lines [8]. It was shown that $Zn_{1-x}Mg_xSe$ under the conditions described in [9] crystallizes in the sphalerite and wurtzite structure for low and high magnesium content, respectively. The phase transition was found to occur at $x = 0.18 \pm 0.03$ [9]. Undoped ZnSe single crystals grown from the vapor phase [10] with a sphalerite structure and orientation [100] were studied for comparison. The measurements were made on crystals with a diameter of around 5–10 mm and a thickness of 1 mm.

The experimental setup for low-temperature measurements of PL and Raman spectra is described in detail in [5]. In the course of the measurements, the sample was immersed into the liquid helium bath of an optical cryostat at a temperature of 4.2 K. The secondary radiation was produced by a He–Ne laser with a wavelength of 632.8 nm and a power of 5 mW or by an Ar^+ laser with a wavelength of 514.5, 488.0, and 476.5 nm and a power of 5, 20, and 5 mW, respectively. In this case, the quantum

energies of the exciting radiation were 1.96, 2.41, 2.54, and 2.60 eV. The secondary radiation spectra were detected by an FEU-79 photomultiplier in the photon counting mode. The width of the instrumental function of the spectrometer used in these experiments was 2–4 cm^{-1} in the spectral range under study. The laser radiation was filtered by a quartz prism and was focused on the sample by a lens or a mirror with a 140-mm focal length. The secondary radiation from the sample was focused by a condenser onto the entrance slit of a DFS-24 double monochromator. The single-electron pulses generated by the photomultiplier were transmitted to the amplifier — a pulse-shaper — then to the discriminator and to the pulse counter, and, finally, to the computer, which in turn controlled the monochromator by means of the control unit. The PL excitation spectra were measured using a halogen lamp as an excitation source in the energy range 1.91–3.10 eV. A narrow part of the halogen lamp radiation spectrum was selected by an MDR-3 monochromator. Infrared absorption in ternary ZnMgSe compounds was investigated within the range from 0.012 eV to 0.122 eV. The IR absorption analysis was carried out using a Bruker 113v Fourier Transform spectrometer with a DTGS detector. The IR measurements were performed at room temperature with a spectral resolution of 0.5 cm^{-1}. A Hg lamp was used as a radiation source.

3. Results and Discussion

The secondary radiation spectra obtained in the backscattering geometry for six $Zn_{1-x}Mg_xSe$ mixed crystals with different composition (x between 0 and 0.49) at a temperature of 4.2 K are presented in Fig. 1 for an excitation photon energy of 2.54 eV. From this figure, one can see that both the Stokes and anti-Stokes components are present in the secondary radiation spectra of each crystal. The anti-Stokes edge emission peak changes its energy position from 2.65 up to 2.98 eV when x increases from 0 to 0.32. The anti-Stokes edge emission is indiscernible in samples with higher values of x. Two deep-level broad PL bands with maxima close to 2.0 and 2.3 eV for $x = 0$ and to 2.2 and 2.5 eV for $x = 0.49$ dominate the spectra. Note that the energy dependence of the PL intensity is virtually continuous when passing from the Stokes to the anti-Stokes PL in the vicinity of the point corresponding to the excitation photon energy marked by the long arrow in Fig. 1. This figure shows that an increase in the magnesium content and consequently in E_g leads to the shift of all PL bands towards higher energy, to weakening of the whole spectrum, and to redistribution of the relative PL-band intensities. The most pronounced redistribution effect is seen as the initial decrease in the intensity of the band with the maximum at 2.3 eV. The intensity of this band decreases with x increasing from 0 to a value of 0.2, close to the point of the sphalerite–wurtzite structure phase transition at $x = 0.18 \pm 0.03$ [9]. This band becomes dominant again in the spectra of the wurtzite-structure compounds at $x \geq 0.32$. The decrease in the secondary-radiation intensity with increasing magnesium content and E_g can be credited mainly to the decrease in absorption of the incident radiation in the bulk of the samples.

According to the previous data for $Zn_{1-x}Mg_xSe$ [8] and ZnSe [1, 3, 7, 11, 12], the edge emission is attributed to the shallow donor–acceptor pair PL. The PL with bands at 1.9–2.0 eV was observed earlier in $Zn_{1-x}Mg_xSe$ [8] and ZnSe [1, 5–7, 10–13] and was attributed to the deep donor–acceptor pair PL in ZnSe. This pair includes deep-level acceptors, which have been assumed to be a complex center incorporating residual impurity of copper [7, 11–13] (Cu(I) center in [12]) or a related intrinsic complex defect self-activated by oxygen (SA(I) center in [12] with a similar structure and a slightly shallower energy level). The attribution of the PL band to donor–acceptor pairs is supported by the results shown in Fig. 2. It illustrates the combined spectral-temporal characteristics of the PL intensity variation obtained with periodic chopping of the exciting beam (opened for 0.5 s and closed for 3 s). In this case, the gratings

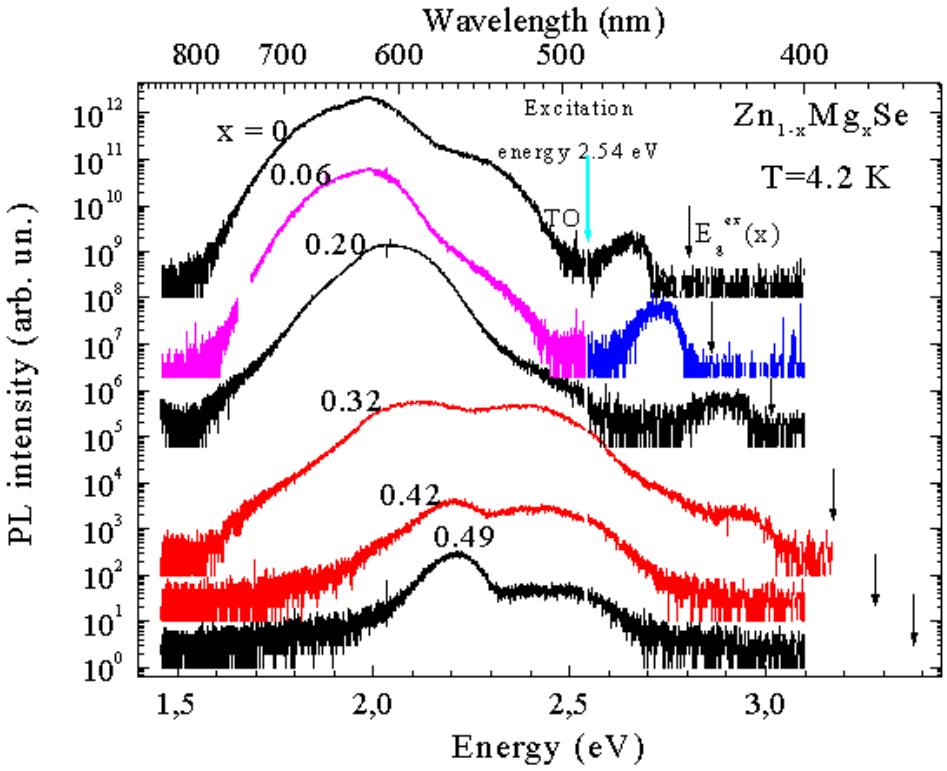

Fig. 1. Emission spectra of $Zn_{1-x}Mg_xSe$ mixed crystals with different compositions x excited by the Ar^+-laser radiation (the 2.54-eV line) at a temperature of 4.2 K. For convenience, the unity levels of the spectra are displaced by multiplication. The arrows indicate the energy gap for the free-exciton state E_g^{ex}.

of the spectrometer were scanned across the spectrum at constant velocity. Thus, the upper envelope of the spectrum in Fig. 2 is similar to the curve presented in Fig. 1, while the lower one corresponds to the intensity distribution of the PL afterglow with a time delay of 3 s after the 0.5-s excitation cutting-off. For the band of 2.0 eV in ZnSe a long-term luminescence (about a few tens of seconds) was observed after the excitation was terminated. The increase in the time delay is accompanied by the peak shift in the spectrum to lower energies. A slow decay and spectral shift are characteristic of the donor–acceptor pair PL. It should be noted that the red afterglow in ZnSe at 4.2 K is eye-detectable for over 1 min.

The band with the maximum at 2.3 eV was also observed earlier in ZnSe [1, 5–7, 10–13] and $Zn_{1-x}Mg_xSe$ [8]. It can be attributed to the residual impurity of copper as well [7, 11–13]. In [12], the origin of this band was described as due to the Cu(II) center. It was attributed to another charge state of the same complex defect as that which was responsible for the Cu(I) center. Morozova et al. [12] argued that the charge state of a Cu(I) center is preferable in II–VI materials with an excess of metal and the charge state corresponding to a Cu(II) center is more probable in materials close to stoichiometry. It should be noted that the intrinsic self-activated complex defect related to the Cu(II) center [12, 13]

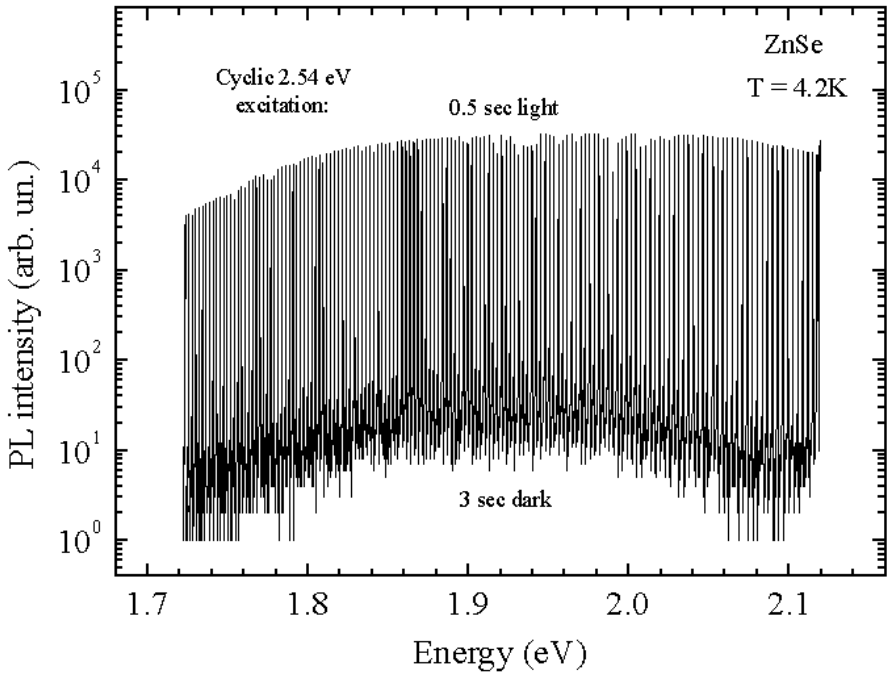

Fig. 2. D–A pair recombination spectrum of the band near 2.0 eV measured at 4.2 K in the Bridgman-grown ZnSe crystal obtained with periodic chopping of the exciting 2.54-eV laser beam (0.5 s of illumination followed by 3 s of darkness).

(SAL(II) center in [12]), the PL band of which appears in ZnSe at 2.5 eV, is poorly detected in the APL spectra of $Zn_{1-x}Mg_xSe$ mixed crystals in Fig. 1.

Figures 3, 4, and 5 show the secondary radiation spectra of three $Zn_{1-x}Mg_xSe$ mixed crystals with composition x equal to 0, 0.06, and 0.32 at a temperature of 4.2 K for four different photon energies of monochromatic exciting radiation (1.96, 2.41, 2.54, and 2.60 eV) with equal excitation power. To estimate the potentiality of the APL technique in the analysis of shallow- and deep-level centers, we have performed similar investigations for the ZnSe crystal grown from the vapor phase. The results are shown in Fig. 6. The bottom parts (b) of Figs. 3–6 show the excitation spectra of the main emission bands represented in the top parts (a) of these figures. The figures show that both the Stokes and anti-Stokes components are present in the spectra of the secondary radiation of every sample for all excitation sources. The comparison of the spectra in Figs. 3–6 shows that the decrease in the excitation photon energy leads to a decrease in the whole spectrum and to redistribution of the relative intensities of the PL bands similar to the results in Fig. 1. Note that the data in Fig. 1 and in Figs. 3–6 are complementary. The spectra in Figs. 3–6 were measured when the excitation photon energy moved across the density of states in the band gap at constant E_g. The data in Fig. 1 correspond to the situation where the features of the density of states move across a constant excitation-photon energy with an increase in E_g. Consequently, Figs. 3–6 resemble the general trends of Fig. 1. The changes in the relative intensity of the PL bands are most pronounced in Figs. 5 and 6 for $Zn_{0.68}Mg_{0.32}Se$ and vapor-grown ZnSe. A less pronounced

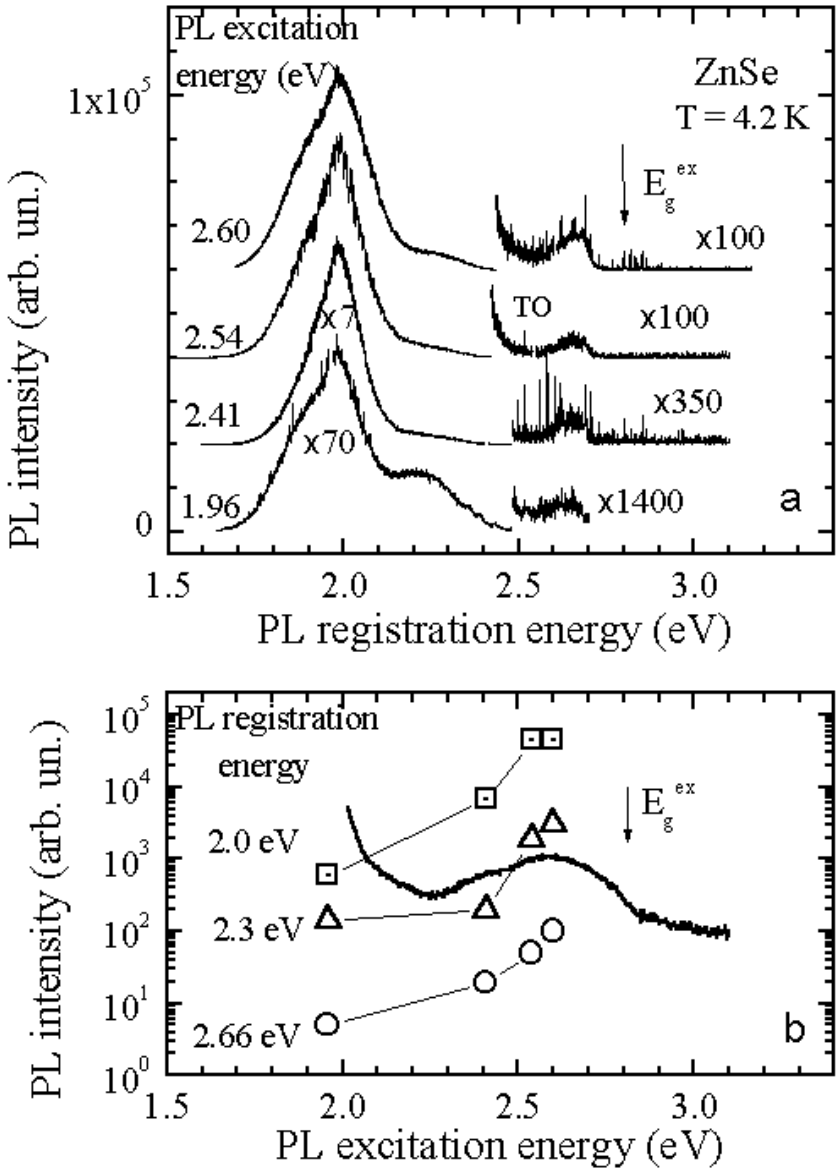

Fig. 3. Emission spectra of the Bridgman-grown ZnSe crystal at 4.2 K under different excitations (a). (The spectrum zero levels are displaced for convenience.) Excitation spectra (shown by symbols) of the PL bands normalized for equal excitation power (b). The solid line corresponds to measurements at the 2.0-eV PL registration energy using a halogen lamp with a monochromator as an excitation source. The arrows indicate the energy gap E_g^{ex}.

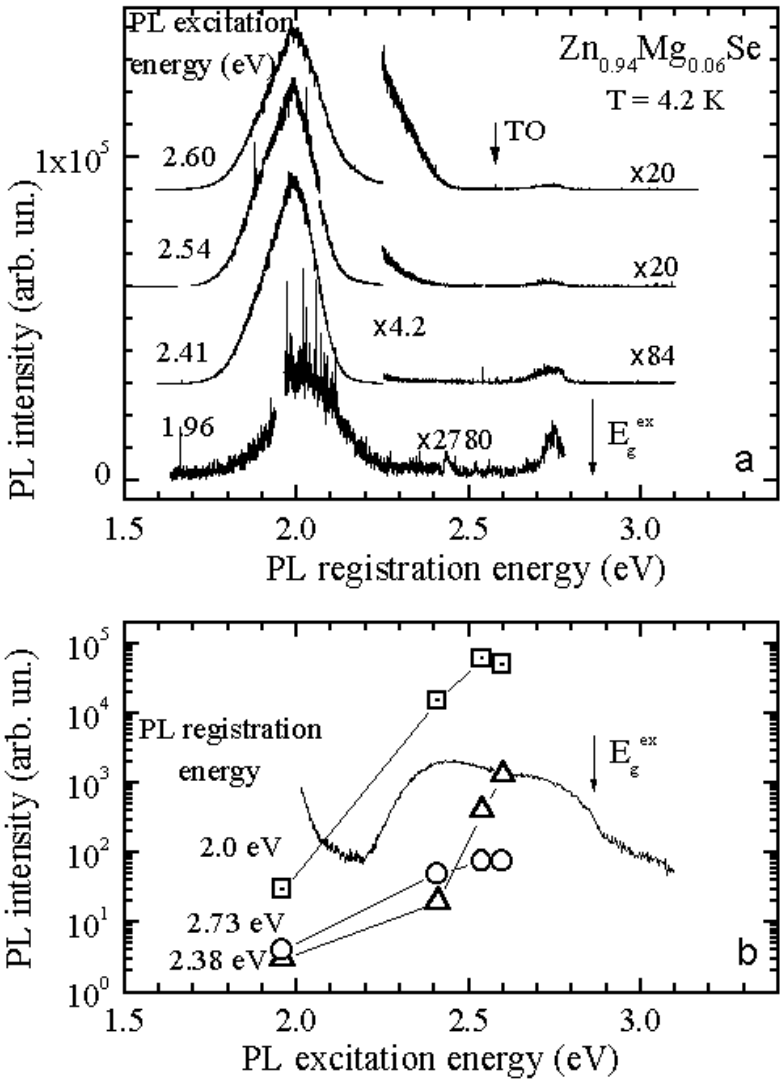

Fig. 4. Emission spectra of the $Zn_{0.94}Mg_{0.06}Se$ mixed crystal at 4.2 K under different excitations. (The spectrum zero levels are displaced for convenience.) Excitation spectra (shown by symbols) of the PL bands normalized for equal excitation power (b). The solid line corresponds to measurements at the 2.0-eV PL registration energy using a halogen lamp with monochromator as an excitation source. The arrows indicate the energy gap $E_g^{\rm ex}$.

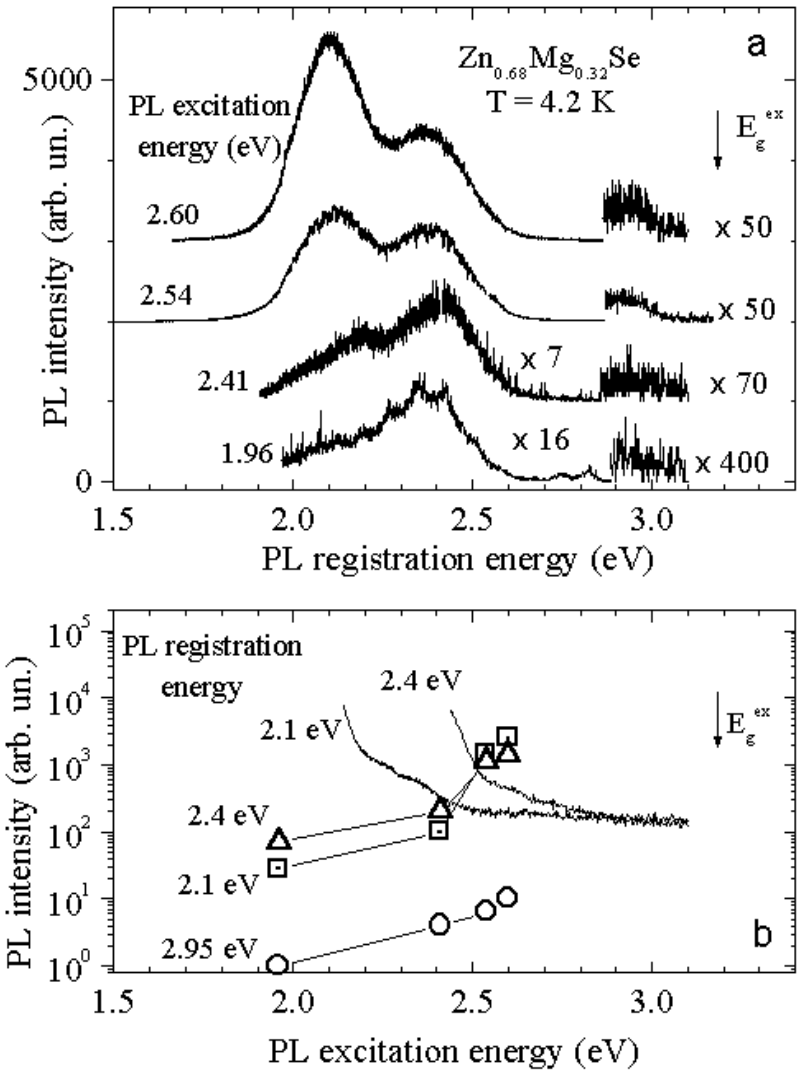

Fig. 5. Emission spectra of the $Zn_{0.68}Mg_{0.32}Se$ mixed crystal at 4.2 K under different excitations (a). (The spectrum zero levels are displaced for convenience.) Excitation spectra (shown by symbols) of the PL bands normalized for equal excitation power (b). The solid lines correspond to measurements at the 2.0-eV PL registration energy using a halogen lamp with monochromator as an excitation source. The arrows indicate the energy gap $E_g^{\rm ex}$.

effect is revealed in Fig. 3 for Bridgman-grown ZnSe. The spectra of the $Zn_{0.94}Mg_{0.06}Se$ crystal in Fig. 4 are almost unchanged except for the increase in the edge-peak relative intensity at the lowest excitation photon energy of 1.96 eV. The decrease in the intensity of the secondary radiation with the decrease in the exciting quantum energy from 2.60 to 1.96 eV can be attributed to the decrease in the absorption coefficient in the bulk of samples analogously to the case in Fig. 1.

From the anti-Stokes luminescence spectra and the spectra of the PL excitation presented in Figs. 3–6 one can conclude the following. The decrease in the excitation energy results in the increase in the relative intensity of higher-energy peaks, including the edge peaks. The excitation of all PL bands in ZnMgSe compounds and ZnSe by quanta with energies of 1.96–2.0 eV occurs mainly via two-stage processes with participation of intermediate levels in the forbidden band. This is also true for the band near 2.0 eV if one takes into account the influence of the Franck–Condon shift. These intermediate levels are in the range of 0.6–2.0 eV above the valence band edge. Such an assumption correlates with the conclusions stated in previous papers [1, 3, 5]. When the energy of the exciting quanta increases, both the two-stage and one-stage processes start to contribute to the excitation of the bands with peaks near 2.0 and 2.3 eV. This results in redistribution of the relative intensity between these bands and the PL peaks of higher energy.

The APL spectra from the bulk of ZnSe crystals grown by different techniques may be compared in Figs. 3 and 6. The data demonstrate the good potentiality of the APL technique in analysis of shallow- and deep-level centers. In the vapor-grown ZnSe crystal the exciton emission (narrow peaks in the range of 2.68–2.8 eV) as well as three broad PL bands with maxima close to 2.0, 2.3, and 2.5 eV resulting from the deep-level center recombination are observed in Fig. 6. The bands with maxima at 2.0 and 2.3 eV are the same as those contained in the spectra of Bridgman-grown ZnSe crystals in Figs. 3 and 1. The band with maximum at 2.5 eV has been discussed above and can be credited to the intrinsic defects [12, 13].

The spectrum of the anti-Stokes secondary radiation (Fig. 6) of vapor-grown ZnSe crystals in the range of 2.60–2.82 eV does not reveal the donor–acceptor pair PL. However, four equidistant sharp maxima appear in this spectral region. According to the available data [14], the high-energy maximum at 2.783 eV is attributed to the so-called I_1^{deep} line of the exciton bound to the deep acceptor. It seems likely [14] that the I_1^{deep} line is due to the complexes containing the Zn vacancies. The equidistant sharp peaks with lower energies in Fig. 6 are the phonon replicas of the I_1^{deep} line with the LO phonon energy of 31.6 meV. The observed difference between the APL spectra of Bridgman-grown and vapor-grown ZnSe crystals in the shallow-level luminescence region points to the distinction in composition of their deep-level centers. Sharp exciton lines have been observed earlier in the spectra of "normal" PL of the $Zn_{1-x}Mg_xSe$ mixed crystals [8] but are not observed in their anti-Stokes luminescence (Figs. 1–5). This behavior can be explained by the difference in the charge state of these materials [15] determined mainly by deep-level centers under the bulk photoexcitation conditions where the density of photogenerated current carriers is much less than that achieved under the "normal" near-surface photoexcitation.

Excitation spectra of the 2.0-eV emission band of mixed crystals measured with a halogen lamp and presented in Figs. 3b and 4b demonstrate the applicability of the volume APL technique to evaluate the band-gap energy. One should analyze the steep increase in luminescence near the band edge caused by the increased transparency of the crystals.

The Stokes components of Raman scattering by LO and TO phonons were observed in $Zn_{1-x}Mg_xSe$ mixed crystals with $x = 0$ and 0.06 together with anti-Stokes photoluminescence at liquid helium temperature under various laser excitations. The investigated $Zn_{1-x}Mg_xSe$ samples were not preliminarily oriented. The occasional orientation of the investigated $Zn_{1-x}Mg_xSe$ crystals was such that both LO and

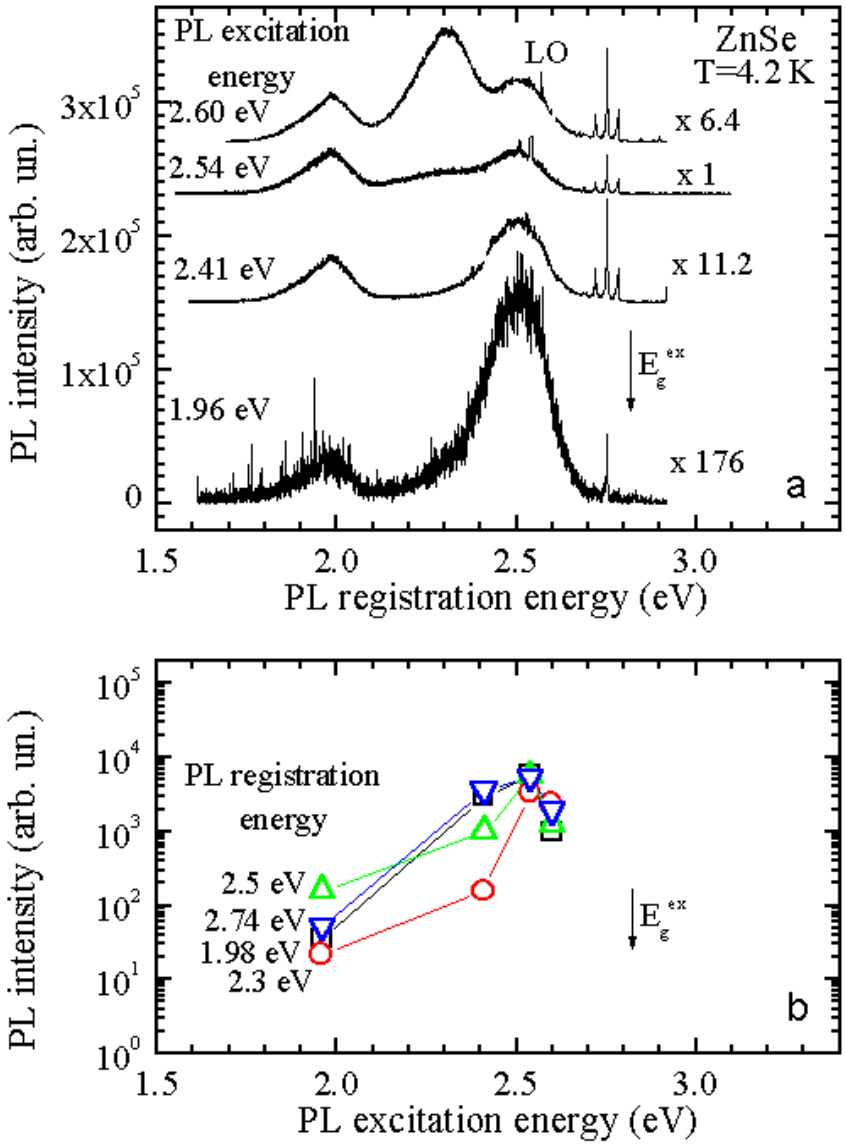

Fig. 6. Emission spectra of a vapor-grown ZnSe crystal at 4.2 K under different excitation quanta (a). (The spectrum zero levels are displaced for convenience.) Excitation spectra (shown by symbols) of the PL bands normalized for constant excitation power (b). The arrows indicate the energy gap E_g^{ex}.

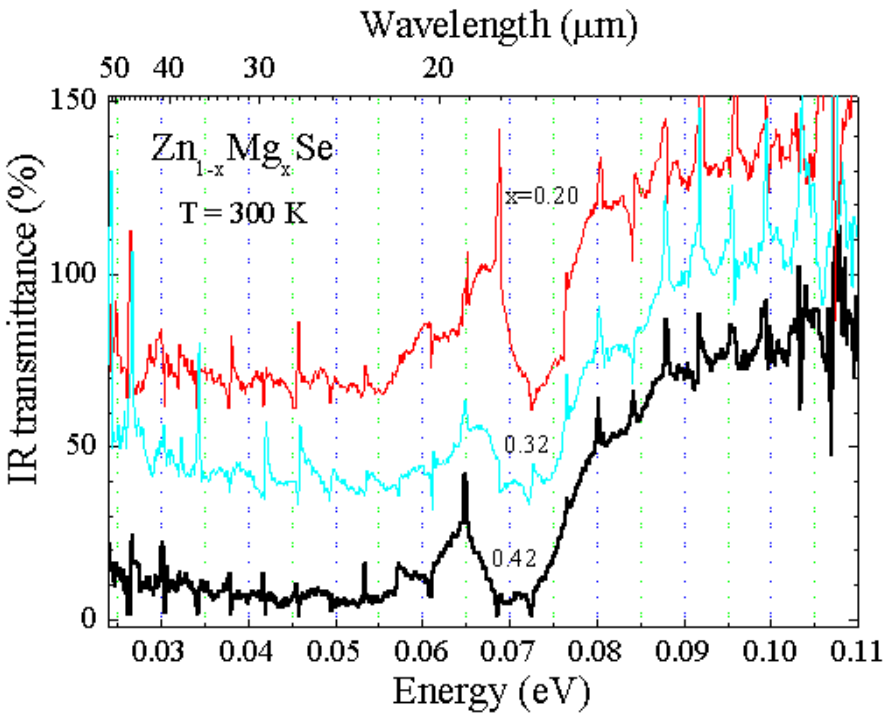

Fig. 7. Room temperature infrared transmittance spectra of $Zn_{1-x}Mg_xSe$ mixed crystals with different composition. The spectra zero levels are 30% displaced for convenience. Periodical sharp features arise due to interference in the sample.

TO Raman components were allowed and observed in the spectrum with an intensity ratio of 1 to 2.4, respectively. Evaluated from Raman measurements, the values of TO and LO phonons corresponding to the ZnSe-mode in $Zn_{1-x}Mg_xSe$ mixed crystals at a temperature of 4.2 K are equal to 25.8 and 31.6 meV for $x = 0$ and 25.65 and 31.4 meV for $x = 0.06$, respectively. The more intense TO-component of Raman scattering is revealed in the spectra in Figs. 1 and 3 as a weak sharp peak that is 26 meV shifted to lower energy from the excitation line. Figure 6 shows Raman light scattering and the emission spectra of a vapor-grown ZnSe crystal at 4.2 K for four different excitation quantum energies in "backscattering" geometry. The only LO component of Raman scattering allowed for the used [100] crystal orientation is visible in the spectra as a sharp peak at 31.6 meV shifted off the excitation line to a lower energy. Comparison of the Raman spectra in the investigated crystals points to the obvious proportionality between the Raman scattering intensity and the APL intensity in close vicinity of the excitation line. This can be connected with the influence of the optical dissipation spectrum of crystals.

Infrared absorption in the three samples of the ternary $Zn_{1-x}Mg_xSe$ compound with composition $x = 0.20$, 0.32, and 0.42 was investigated at room temperature. The IR transmission is shown in Fig. 7. The transmission drop of lower photon energies is due to the fundamental absorption near 25 meV. The most pronounced effect in the IR spectra is the shift of the absorption band ∼70 meV to the lower

energies with increasing magnesium content x. This absorption band can be attributed to the TO+TO combination band [16] of the MgSe-mode in ternary $Zn_{1-x}Mg_xSe$ compounds. The observed shift is in good agreement with the data of Raman measurements for the MgSe-mode of TO phonons [17].

4. Conclusions

This work presents the results of investigations on photoluminescence and Raman scattering in ZnSe and ternary $Zn_{1-x}Mg_xSe$ compounds at 4.2 K. The crystals were excited by laser radiation with a photon energy lower than the energy gap and with a relatively low power from 5 to 20 mW. The investigated ternary $Zn_{1-x}Mg_xSe$ crystals were obtained by the modified Bridgman method and ZnSe crystals obtained by vapor growth. The anti-Stokes luminescence was observed for the first time in the ternary $Zn_{1-x}Mg_xSe$ compounds. For all investigated samples the corresponding transformation of the Stokes and anti-Stokes emission was measured. The sharp exciton lines observed in the vapor-grown ZnSe crystals are not observed in the anti-Stokes luminescence of the mixed crystals. This behavior can be explained by the difference in the charge state of these materials under conditions of the bulk photoexcitation. We assume that the anti-Stokes emission is related to the mechanism of two-step excitation via deep-level centers.

The presented technique of the volume excitation of the low-temperature secondary radiation can be used in qualitative and quantitative analysis of both shallow- and deep-level centers in the bulk of a semiconductor, in particular under the conditions of extremely low concentrations of non-equilibrium photogenerated carriers, which are undetectable in the case of ordinary near-surface photoluminescence.

Acknowledgments

The work was supported by the Russian Foundation for Basic Research (Project Nos. 02-02-16221 and 02-02-16977), the State Research Program on Physics and Technology of Nanostructures (Project No. 97-1048), and the Federal Target Program "Integratsiya" (Project No. B0049).

References

1. I. Broser and R. Broser-Warminsky, "Anti-Stokes luminescence of zinc sulfide type phosphorus," in: H. P. Kallmann and G. M. Spruch (Eds.), *Luminescence of Organic and Inorganic Materials*, Wiley, New York (1962), p. 402.
2. Yu. P. Chukova, *Anti-Stokes Luminescence and New Possibilities for Its Application* [in Russian], Sovetskoe Radio, Moscow (1980).
3. V. Yu. Ivanov, Yu. G. Semenov, M. Surma, and M. Godlewski, *J. Luminesc.*, **72–74**, 101 (1997).
4. M. D. Galanin, *Luminescence of Molecules and Crystals*, Interscience Publishing, Cambridge (1996).
5. V. S. Gorelik, A. L. Karuzskii, Yu. V. Klevkov, et al., "Raman scattering and anti-Stokes luminescence in wide gap semiconductors," in: V. S. Gorelik and A. D. Kudryavtseva (Eds.), *Raman Scattering*, *Proc. SPIE*, **4069**, 83 (2000).
6. V. S. Gorelik, A. L. Karuzskii, P. P. Sverbil, and A. V. Chervyakov, *J. Russ. Laser Res.*, **23**, 459 (2002).
7. A. N. Georgobiani and M. K. Sheinkman (Eds.), *Physics of $A^{II}B^{VI}$ Compounds* [in Russian], Nauka, Moscow (1986).

8. F. Firszt, H. Męczyńska, B. Sekulska, et al., *Semicond. Sci. Technol.*, **10**, 197 (1995).
9. F. Firszt, S. Łęgowski, H. Męczyńska, et al., *Acta Phys. Pol.* A, **88**, 711 (1995).
10. Yu. V. Korostelin, V. I. Kozlovsky, A. S. Nasibov, and P. V. Shapkin, *J. Crystal Growth*, **161**, 51 (1996).
11. V. I. Gavrilenko, A. M. Grekhov, D. V. Korbutyak, and V. G. Litovchenko, *Optical Properties of Semiconductors* [in Russian], Naukova Dumka, Kiev (1987).
12. N. K. Morozova, I. A. Karetnikov, V. V. Blinov, and E. M. Gavrishchuk, *Semiconductors*, **35**, 24 (2001).
13. M. Aven and J. S. Prenner (Eds.), *Physics and Chemistry of II–VI Compounds*, North Holland, Amsterdam (1967).
14. E. Tournié, C. Morhain, G. Neu, et al., *Appl. Phys. Lett.*, **68**, 1356 (1996).
15. M. Chiba, V. A. Fradkov, A. L. Karuzskii, et al., *Physica B: Cond. Matt.*, **302**, 408 (2001).
16. D. A. Kleinman and W. G. Spitzer, *Phys. Rev.*, **118**, 110 (1960).
17. F. Firszt, S. Łęgowski, H. Męczyńska, et al., "Photoluminescence, cathodoluminescence, and Raman investigations of $Zn_{1-x}Mg_xSe$ mixed crystals," in: J. Żmija, A. Majchrowski, J. Rutkowski, J. Zieliński (Eds.), *Solid State Crystals: Growth and Characterization*, *Proc. SPIE*, **3178**, 213 (1997).